THE JOURNAL OF BIOLOGICAL CHEMISTRY
Vol. 279, No. 23, Issue of June 4, pp. 24444–24451, 2004
Printed in U.S.A.


# Human Mob Proteins Regulate the NDR1 and NDR2 Serine-Threonine Kinases*

Received for publication, February 24, 2004, and in revised form, April 1, 2004
Published, JBC Papers in Press, April 2, 2004, DOI 10.1074/jbc.M401999200

**Eric Devroe‡, Hediye Erdjument-Bromage§, Paul Tempst§, and Pamela A. Silver‡¶**

*From the ‡Department of Systems Biology, Harvard Medical School and Department of Cancer Cell Biology, The Dana-Farber Cancer Institute, Boston, Massachusetts 02115 and §Molecular Biology Program, Memorial Sloan-Kettering Cancer Center, New York, New York 10021*

**Human NDR1 (nuclear Dbf2-related) is a widely expressed nuclear serine-threonine kinase that has been implicated in cell proliferation and/or tumor progression. Here we present molecular characterization of the human NDR2 serine-threonine kinase, which shares ~87% sequence identity with NDR1. *NDR2* is expressed in most human tissues with the highest expression in the thymus. In contrast to NDR1, NDR2 is excluded from the nucleus and exhibits a punctate cytoplasmic distribution. The differential localization of NDR1 and NDR2 suggests that each kinase may serve distinct functions. Thus, to identify proteins that interact with NDR1 or NDR2, epitope-tagged kinases were immunoprecipitated from Jurkat T-cells. Two uncharacterized proteins that are homologous to the *Saccharomyces cerevisiae* kinase regulators Mob1 and Mob2 were identified. We demonstrate that NDR1 and NDR2 partially colocalize with human Mob2 in HeLa cells and confirm the NDR-Mob interactions in cell extracts. Interestingly, NDR1 and NDR2 form stable complexes with Mob2, and this association dramatically stimulates NDR1 and NDR2 catalytic activity. In summary, this work identifies a unique class of human kinase-activating subunits that may be functionally analagous to cyclins.**

Mammalian genomes encode two highly related serine-threonine kinases, NDR1[1] (nuclear Dbf2-related) and NDR2. Human NDR1 (GenBank™ accession number NP_009202) was named based on its homology to the yeast Dbf2 kinase and characterized as a nuclear serine-threonine kinase expressed in all human tissues with the exception of the brain (1). Human NDR1 and *Saccharomyces cerevisiae* Dbf2 activity can be dramatically stimulated by okadaic acid, suggesting that the NDR family of kinases require phosphorylation for proper activation (2, 3). Indeed, $Ca^{2+}$ induces NDR1 autophosphorylation as well as phosphorylation by an unidentified upstream kinase (4). NDR1 activity is also regulated by interaction with $Ca^{2+}$/S100 calcium-binding proteins (5).

Although its precise function(s) remain unclear, evidence suggests that NDR1 may be involved in cell proliferation and/or tumor progression. First, NDR1 is hyperactivated in several S100B-positive melanoma cell lines (5). Given that S100B is overexpressed in greater than 80% of metastatic melanomas (6), NDR1 activity may influence tumor metastatic potential. Second, microdissection and gene expression profiling reveal that *NDR1* mRNA is up-regulated 1.9-fold in high *versus* low risk ductal carcinoma *in situ* (7). Despite these intriguing observations, NDR1 has no known substrates and has not been implicated in any signal transduction pathway.

Substrate identification has undoubtedly been hampered by the seemingly low enzymatic activity of NDR1. Indeed, NDR1 expressed in either *Escherichia coli* or COS-1 cells is unable to transphosphorylate "generic" kinase substrates such as histone H1, myelin basic protein (MBP), casein, or phosvitin (1). Nevertheless, purified human NDR1 possesses catalytic activity. By screening a small peptide library, Hemmings and colleagues (5) identify a short peptide (KKRNRRLSVA) that serves as an NDR1 substrate. Taken together, these data suggest that either NDR1 has a very stringent substrate specificity or we have insufficient biological insight to purify active preparations of NDR1.

Mammalian genomes encode a related kinase, NDR2 (GenBank™ accession number NP_055815), which is ~87% identical to NDR1 at the amino acid level (4, 8). Currently, the NDR2 kinase remains uncharacterized. However, a recent retroviral insertional mutagenesis study found that the murine *NDR2* gene (also known as serine-threonine kinase 38-like) was disrupted in two independent B-cell lymphomas (9). This result suggests that NDR2 may also be involved in tumor initiation or progression. Given their potential involvement in cancer, we sought to characterize the human NDR1 and NDR2 kinases. In this study, we identified and characterized two new NDR1 and NDR2 binding partners, Mob1B and Mob2.

## EXPERIMENTAL PROCEDURES

*Cell Culture*—HeLa and 293T cells were maintained in Dulbecco's modified Eagle's medium containing 10% fetal bovine serum, 5 units/ml penicillin, and 5 μg/ml streptomycin. HeLa cells were transiently transfected using FuGENE 6 transfection reagent (Roche Applied Science) as described previously (10). Fluorescence microscopy and indirect immunofluorescence microscopy were performed on a DeltaVision platform (Applied Precision Inc.) as described previously (10). 293T cells were transiently transfected with calcium phosphate. Jurkat T-cells were maintained in RPMI 1640 medium containing 10% fetal bovine serum and penicillin/streptomycin.

*Plasmids*—The full-length *NDR1* and *NDR2* open reading frames (ORFs) were amplified by PCR from cDNA prepared from total HeLa RNA. The *NDR1* ORF was cloned into the pECMV-FLAG (10) or pEGFP-C1 vector (Clontech) to generate pFLAG-NDR1 and pGFP-

* This work was supported by a Howard Hughes Medical Institute predoctoral fellowship (to E. D.), a NCI Cancer Center Support grant from the National Institutes of Health (to P. T.), and the Claudia Adams Barr Fund and Novartis/Dana-Farber Cancer Institute Drug Discovery Program (to P. A. S.). The costs of publication of this article were defrayed in part by the payment of page charges. This article must therefore be hereby marked "*advertisement*" in accordance with 18 U.S.C. Section 1734 solely to indicate this fact.

¶ To whom correspondence should be addressed. Tel.: 617-632-5102; Fax: 617-632-5103; E-mail: pamela_silver@dfci.harvard.edu.

[1] The abbreviations used are: NDR, nuclear Dbf2-related; MBP, myelin basic protein; ORF, open reading frame; KD, kinase-dead; GFP, green fluorescent protein; MALDI-reTOF, matrix-assisted laser desorption ionization reflectron time-of-flight; MS, mass spectrometry; *HCCA2*, hepatocellular carcinoma-associated gene 2; WT, wild-type; sc, *S. cerevisiae*; MSCV, murine stem cell virus; LEDGF, lens epithelial-derived growth factor.

NDR1, respectively. Similarly, the NDR2 ORF was cloned into the pECMV-FLAG or pEGFP-C1 vector to generate pFLAG-NDR2 and pGFP-NDR2. Kinase-dead (KD) derivatives were generated by PCR using the QuikChange mutagenesis kit (Stratagene) with oligonucleotides that change the invariant Lys to Ala (K118A for NDR1, K119A for NDR2). Retroviral vectors were also constructed by cloning FLAG-NDR1 or FLAG-NDR2 ORFs into the murine stem cell virus (MSCV) vector pMSCV-puro (Clontech), generating pMSCV-FLAG-NDR1 and pMSCV-FLAG-NDR2. Retroviruses were packaged as described previously (11). Full-length *Mob1B* and *Mob2* ORFs were amplified by PCR from cDNA prepared from Jurkat total RNA and inserted into pEGFP-C1 to generate pGFP-Mob1B and pGFP-Mob2, respectively.

*Northern and Western Blot Analyses*—To generate unique *NDR1* and *NDR2* probes, a ~350-bp region at the 3′ end of each cDNA was gel-purified and labeled with a Rediprime II labeling system (Amersham Biosciences). Radiolabeled probes were hybridized to a FirstChoice™ Northern Human Blot I membrane (Ambion) in UltraHyb (Ambion), washed to a stringency of 0.2× SSC, 0.1% SDS at 42 °C, and exposed to a PhosphorImager (Amersham Biosciences). Western blot analysis was performed as described previously (11) using monoclonal anti-FLAG M2 (Sigma), monoclonal anti-NDR1 (BD Transduction Laboratories), monoclonal anti-p75/LEDGF (BD Transduction Laboratories), or polyclonal anti-GFP. BenchMark™ protein ladder (Invitrogen) was used as a molecular weight standard for SDS-PAGE and Western blot analysis.

*Identification of NDR1- and NDR2-interacting Proteins*—Jurkat T-cells were infected with MSCV, MSCV-FLAG-NDR1, or MSCV-FLAG-NDR2 and expanded in the presence of 1 μg/ml puromycin. Whole cell extracts were prepared in immunoprecipitation buffer (50 mM HEPES, pH 7.5, 500 mM NaCl, 0.5% Triton X-100, 5% glycerol, 20 mM B-glycerophosphate, 1 mM sodium orthovanadate containing Complete protease inhibitors (Roche Applied Science)) and clarified by ultracentrifugation (20,000 rpm for 1.5 h at 4 °C using a Ti-70 rotor). Lysates were immunoprecipitated with anti-FLAG M2 affinity matrix (Sigma), washed extensively, and eluted with the FLAG peptide.

Immunoprecipitated protein were resolved by 4–20% Tris-glycine Novex SDS-PAGE and stained with Simply Blue (Invitrogen). The gel-resolved proteins were digested with trypsin, the mixtures were fractionated on a Poros 50 R2 RP microtip, and the resulting peptide pools were analyzed by matrix-assisted laser desorption ionization reflectron time-of-flight (MALDI-reTOF) mass spectrometry (MS) using a BRUKER UltraFlex TOF/TOF instrument (Bruker Daltonics) as described previously (12, 13). Selected experimental masses (*m/z*) were taken to search a nonredundant protein data base (~$1.4 \times 10^6$ entries, National Center for Biotechnology Information) utilizing the PeptideSearch (Matthias Mann, Southern Denmark University) algorithm with a mass accuracy restriction better than 40 ppm and no more than one missed cleavage site allowed per peptide. Mass spectrometric sequencing of selected peptides was done by MALDI-TOF/TOF (MS/MS) analysis on the same prepared samples using the UltraFlex instrument in the "LIFT" mode. Fragment ion spectra were taken to search nonredundant using the MASCOT MS/MS ion search program (Matrix Science Ltd.). Thus, any identification obtained was verified by comparing the computer-generated fragment ion series of the predicted tryptic peptide with the experimental MS/MS data. Hsp90α/β (GenBank™ accession numbers P07900 and NP_031381, respectively) were identified as the ~95-kDa band coimmunoprecipitating with FLAG-NDR1. Mob1B (GenBank™ accession number NP_775739; currently annotated as Mob4A yet referred to as Mob1B by Stavridi *et al*. (14)) was identified as the ~26-kDa protein coimmunoprecipitating with FLAG-NDR2. Mob2 (GenBank™ accession number NP_443731) was identified as the ~30-kDa protein coimmunoprecipitating with both FLAG-NDR1 and FLAG-NDR2. Of note, these tryptic peptides also matched to an unknown protein product of ~16 kDa (BAB71443), but the mobility of the immunoprecipitated protein was much more consistent with Mob2 (~27 kDa). A sequence analysis indicates that BAB71443 is an alternately spliced variant of Mob2 (data not shown).

*NDR1 and NDR2 Kinase Reactions*—293T cells were transiently transfected with either pFLAG-NDR1 or pFLAG-NDR2 and pEGFP-C1, pGFP-Mob1B, or pGFP-Mob2. When indicated, the transfected cells were pulsed with 1 μM okadaic acid (Calbiochem) for 1 h prior to harvesting. At ~45-h post-transfection, cells were washed with cold phosphate-buffered saline and then lysed in buffer containing 50 mM HEPES, pH 7.9, 1% Triton X-100, 250 mM NaCl, 50 mM NaF, 25 mM B-glycerophosphate, 1 mM sodium orthovanadate, and Complete protease inhibitors. Lysates were clarified by ultracentrifugation. Prior to immunoprecipitation, salt content was normalized to 500 mM NaCl. FLAG-NDR1 or FLAG-NDR2 complexes were immunoprecipitated with anti-FLAG M2 affinity resin, washed extensively in the above lysis buffer containing 500 mM NaCl and 0.1% Triton X-100, and then eluted in 50 mM HEPES, pH 7.9, 20% glycerol, 0.05% Triton X-100, 100 mM NaCl, 50 mM NaF, 25 mM B-glycerophosphate, 1 mM sodium orthovanadate, Complete protease inhibitors, and 200 μg/ml FLAG peptide (Sigma) and stored at −80 °C. *In vitro* kinase reactions were performed by incubating enzyme preparation in 25 mM HEPES, pH 7.9, 10 mM $MgCl_2$, 1 mM dithiothreitol, and 100 μM [$\gamma$-$^{32}$P]ATP (~1 μCi/μl) for 1 h at 30 °C. Transphosphorylation assays included 10 μg of dephosphorylated MBP (Upstate Biotechnology) and were performed for 20 min at 30 °C. Reactions were stopped by the addition of cold 2× SDS sample buffer. Samples were resolved by 12% SDS-PAGE, stained with Simply Blue, and exposed to a PhosphorImager.

*Protein Alignments*—The ClustalW algorithm was used to align the indicated protein sequences (15). Alignments were formatted with the ESPript tool (16).

## RESULTS

*Tissue Expression and Subcellular Localization of NDR1 and NDR2*—The human NDR1 and NDR2 kinases are ~87% identical at the amino acid level (Fig. 1*A*). Most of the nonidentical residues cluster at the N and C termini of the enzymes, and these differences are highly conserved in the murine NDR1 and NDR2 sequences. Residues known to regulate NDR1 activity including Thr-74, Ser-281, and Thr-444 (reviewed in Ref. 8) are conserved in NDR2 and correspond to NDR2 residues Thr-75, Ser-282, and Thr-442. The NDR1 S100B-binding domain (residues 62–86) (5) contains one conservative and one nonconservative change in NDR2 (residues 63–87), whereas the NDR1 nuclear localization signal (residues 265–276) (1) contains a single conservative change in NDR2 (residues 266–277).

To gain insight into NDR2 biology, we initially characterized its tissue distribution and subcellular localization. Northern blot analysis revealed that *NDR2*, similar to *NDR1* (1), was expressed in most human tissues and was particularly abundant in the thymus (Fig. 1*B*). We next cloned the full-length *NDR1* and *NDR2* ORFs into expression vectors encoding an N-terminal FLAG or GFP tag. HeLa cells were transiently transfected with these expression vectors, and NDR1 and NDR2 subcellular localization was monitored by fluorescence microscopy or indirect immunofluorescence microscopy. FLAG-NDR1 and GFP-NDR1 proteins had accumulated in the nucleus but were also detected in the cytoplasm (Fig. 1*C*). In contrast, FLAG-NDR2 and GFP-NDR2 proteins were predominantly excluded from the nucleus and exhibited a punctate cytoplasmic distribution (Fig. 1*C*). Hemmings and colleagues (1) have previously characterized NDR1 amino acid residues 265–276 (KRKAETWKRNRR) as an nuclear localization signal, because the deletion of this basic peptide had mislocalized hemagglutinin-NDR1 to the cytoplasm in transiently transfected COS-1 cells (1). Because NDR2 contains only a single conservative mutation in this region (KRN to KKN) (see Fig. 1*A*), it is intriguing that NDR2 predominantly accumulated in the cytoplasm. Incubation of transiently transfected cells with leptomycin B, a specific Crm1-dependent nuclear export inhibitor, did not alter the intracellular distribution of either kinase, suggesting that differences in nuclear import/export kinetics were not likely to explain their differential compartmentalization at steady state (data not shown). Finally, we compared the localization of epitope-tagged NDR1 to endogenous NDR1. Biochemical fractionation and Western blotting indicated that endogenous NDR1 was localized to both the nucleus and the cytoplasm (Fig. 1*C*, *lower panel*), which is consistent with our FLAG-NDR1 and GFP-NDR1 analyses.

*Mob Proteins Coimmunoprecipitate with NDR1 and NDR2*—To identify proteins that interact with NDR1 and NDR2, we generated Jurkat T-cell lines stably expressing FLAG-NDR1 or FLAG-NDR2. Following affinity purification, eluted samples were resolved by SDS-PAGE (Fig. 2*A*). Specific bands were

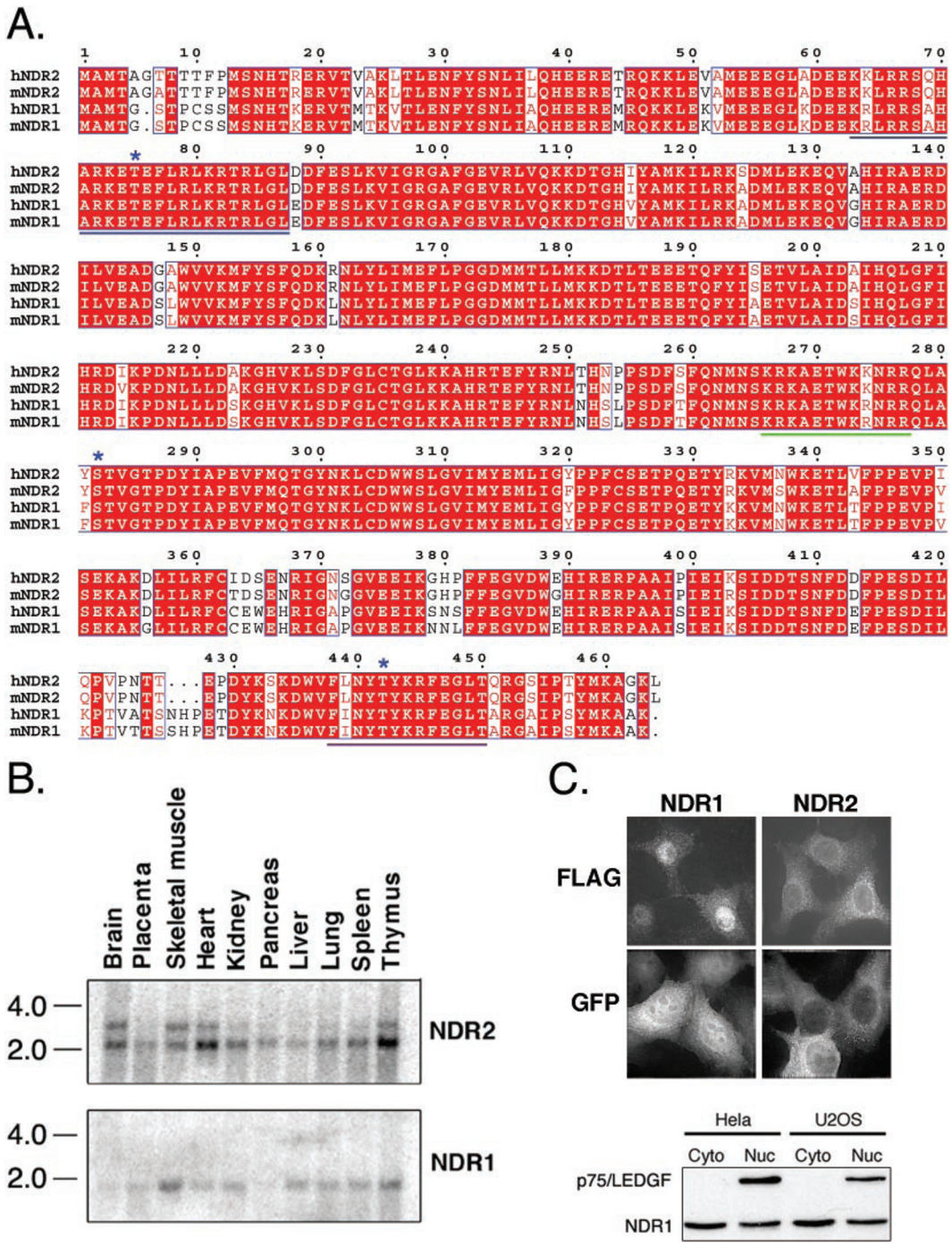


FIG. 1. **Characterization of NDR1 and NDR2.** *A*, multiple sequence alignment of the human (*h*) and murine (*m*) NDR1 and NDR2 serine-threonine kinases. Identical residues are shown in *white font* with a *red background*. Conserved residues are shown in *red*, whereas nonconserved residues are shown in *black*. Gaps are indicated by *dots*. Residues known to affect human NDR1 activity (8) are emphasized with a *blue asterisk*. The NDR1 S100B-binding domain, nuclear localization signal, and hydrophobic motif (8) are emphasized with a *blue*, *green*, and *purple line* under the relevant residues. *B*, Northern blot analysis of *NDR1* and *NDR2* mRNA expression. A FirstChoice Northern human blot I membrane (Ambion) was probed with radiolabeled *NDR1*- or *NDR2*-specific cDNA probes. The approximate positions of millenium marker standards in kb are shown to the *left*. *C*, subcellular localization of NDR1 and NDR2. HeLa cells were transiently transfected with pFLAG-NDR1, pFLAG-NDR2, pGFP-NDR1, or pGFP-NDR2 and observed 20-h post-transfection by fluorescence microscopy (*GFP*) or indirect immunofluorescence microscopy with the anti-FLAG M2 antibody (*FLAG*). Below, nuclear (*Nuc*) and cytosolic (*Cyto*) extracts from HeLa and U2OS cells were analyzed by Western blotting using anti-NDR1 and anti-p75/LEDGF antibodies. p75/LEDGF is restricted to the nucleus, whereas NDR1 is detected in both nuclear and cytosolic fractions.

excised from the gel, and the indicated proteins were identified by a combination of peptide mass fingerprinting using MALDI-TOF MS and mass spectrometric sequencing using MALDI-TOF/TOF MS/MS. We identified the ~95-kDa band detected in NDR1 immunoprecipitations as Hsp90$\alpha$ (GenBank$^{TM}$ accession number P07900) and Hsp90$\beta$ (GenBank$^{TM}$ accession number NP_031381). However, these proteins were also identified in Mock samples, suggesting that Hsp90$\alpha/\beta$s partially adhere nonspecifically to the anti-FLAG resin under these conditions.

Aside from Hsp90$\alpha/\beta$, we identified the ~30-kDa band coimmunoprecipitating with both NDR1 and NDR2 as Mob2 (Fig. 2*A*) and the ~26-kDa band coimmunoprecipitating with NDR2 as Mob1B. Of note, the ~26-kDa band is not visible on the scanned Simply Blue-stained gel (*top panel*) but was readily

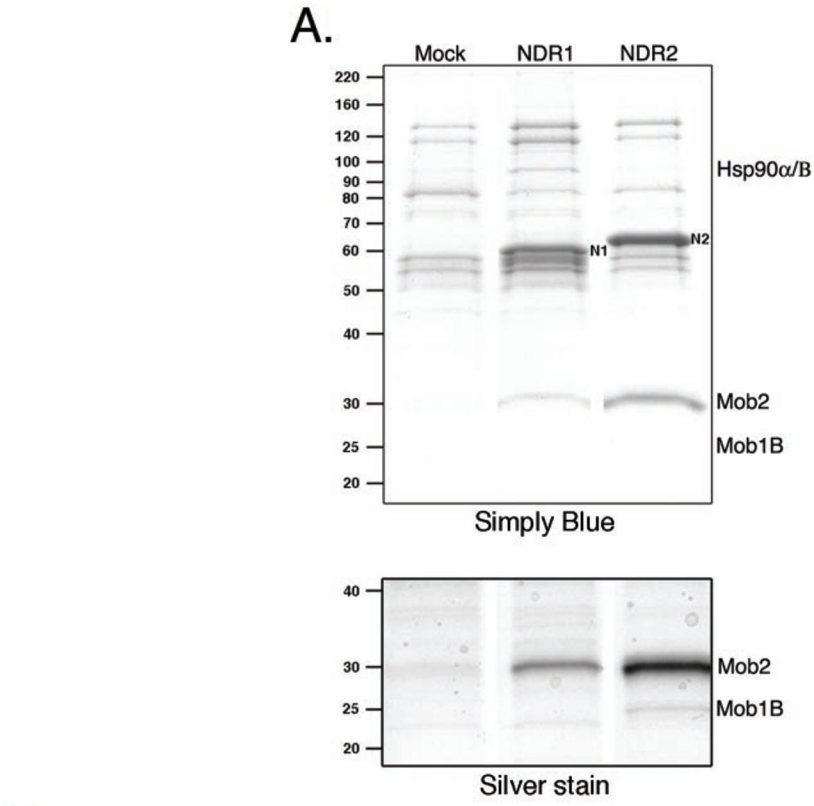


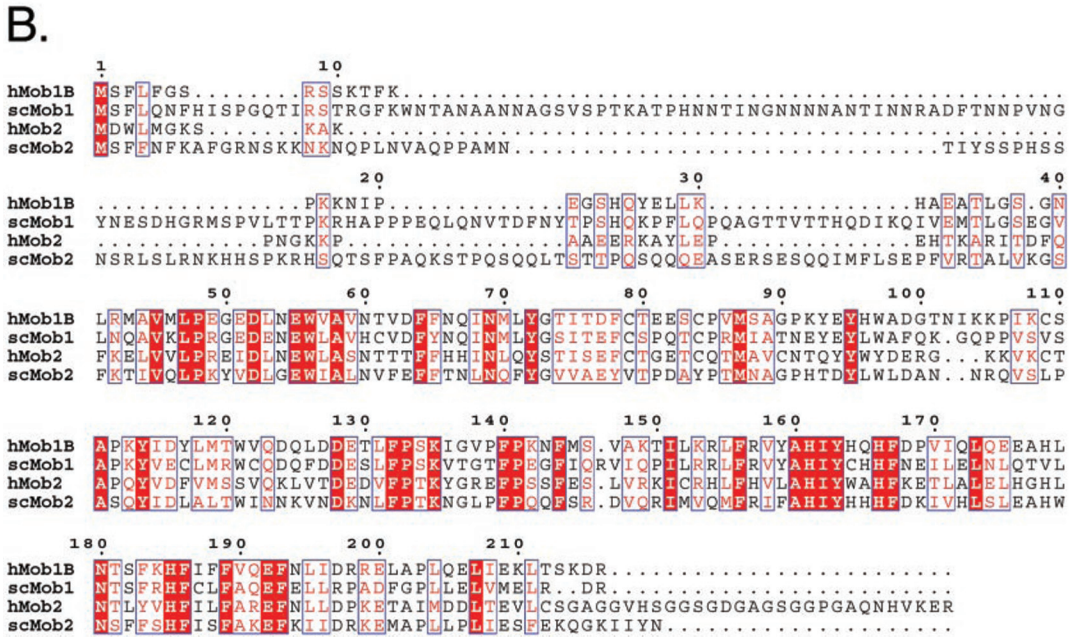


FIG. 2. **Identification of NDR1- and NDR2-interacting proteins.** *A*, extracts were prepared from Jurkat T-cells infected with an empty retroviral cassette (*Mock*) or retroviral vectors encoding FLAG-NDR1 (*NDR1*) or FLAG-NDR2 (*NDR2*) and immunoprecipitated with anti-FLAG M2 affinity resin. Bound proteins were eluted with the FLAG peptide, resolved by SDS-PAGE, and stained with Simply Blue. The position of molecular mass markers in kDa is shown. The position of FLAG-NDR1 (N1) and FLAG-NDR2 (N2) are indicated as well as the coimmunoprecipitating Mob2 and Mob1B proteins. The ~26-kDa Mob1B protein coimmunoprecipitated with NDR2 is not visible on the scanned Simply Blue-stained gel (*top panel*) but was readily observable following silver staining (*bottom panel*). Aside from the Mob proteins, Hsp90$\alpha$ and Hsp90$\beta$ were detected in the NDR1 immunoprecipitation. However, Hsp90$\alpha$ and Hsp90$\beta$ were also detected in the Mock sample, indicating that these proteins partially adhere nonspecifically to the anti-FLAG resin under these conditions. *B*, multiple sequence alignment of human (*h*) Mob1B and Mob2 and the scMob1 and scMob2 proteins. Identical residues are shown in *white font* with a *red background*, conserved residues are shown in *red*, whereas nonconserved residues are shown in *black*. Gaps are indicated by *dots*.

observable following silver staining (*bottom panel*). A sequence analysis demonstrated that the identified proteins are homologous to the *S. cerevisiae* Mob1 and Mob2 proteins (Fig. 2*B*).

*Mob2 Colocalizes with NDR1 and NDR2*—We first sought to characterize the localization of Mob1B, the ~26-kDa protein that was faintly detected in NDR2 immunoprecipitations (Fig. 2*A*). To this end, the full-length *Mob1B* ORF was cloned into an expression vector in-frame with an N-terminal GFP tag. GFP-Mob1B localization was then examined by fluorescence microscopy in transiently transfected HeLa cells. Mob1B exhibited

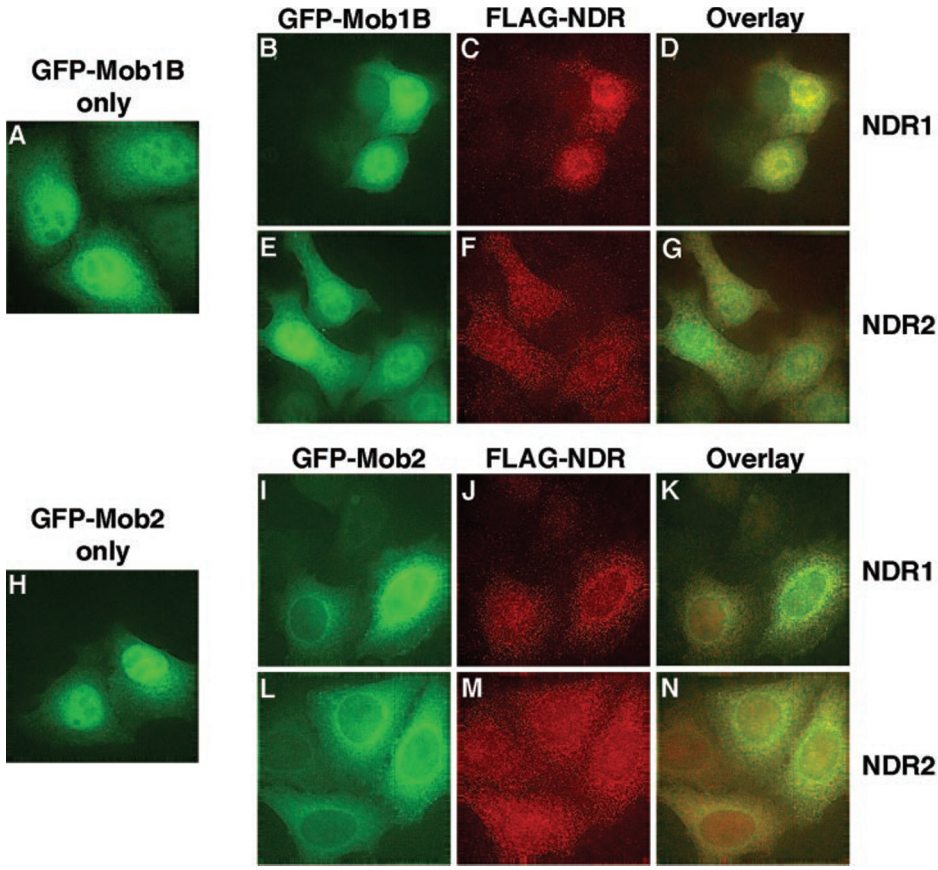


FIG. 3. **NDR1 and NDR2 colocalize with Mob2.** HeLa cells transiently transfected with pGFP-Mob1B alone (*A*) or cotransfected with pGFP-Mob1B and pFLAG-NDR1 (*B–D*) or pFLAG-NDR2 (*E–G*) were analyzed by fluorescence and indirect immunofluorescence microscopy. A representative field of view illustrating Mob1B (*A*, *B*, and *E*), NDR1 (*C*), and NDR2 (*F*) localization is shown. The merged images (*D* and *G*) demonstrate that NDR1 and NDR2 partially colocalize with Mob1B, yet interpretation of these data is difficult given the pan-cellular distribution of Mob1B. Similarly, HeLa cells transiently transfected with pGFP-Mob2 alone (*H*) or cotransfected with pGFP-Mob2 and pFLAG-NDR1 (*I–K*) or pFLAG-NDR2 (*L–N*) were analyzed by fluorescence and indirect immunofluorescence microscopy. A representative field of view illustrating Mob2 (*H*, *I*, and *L*), NDR1 (*J*), and NDR2 (*M*) localization is shown. Note that coexpression of NDR1 or NDR2 with Mob2 results in Mob2 relocalization (compare *H* with *I* and *L*). NDR1 localization also changes upon coexpression (compare *C* with *J*). The merged images (*K* and *N*) demonstrate that NDR1 and NDR2 partially colocalize with Mob2, particularly in regions surrounding the nucleus.

both nuclear and diffuse cytoplasmic distribution when expressed alone (Fig. 3*A*). Coexpression of NDR1 (Fig. 3, *B–D*) or NDR2 (Fig. 3, *E–G*) did not noticeably alter the distribution of Mob1B. Consistent with our earlier observations (Fig. 1*C*), NDR1 localized predominantly to the nucleus with less prominent cytoplasmic speckles (Fig. 3*C*). NDR2 exhibited heterogeneous cellular distribution with predominantly cytoplasmic speckles (Fig. 3*F*). Although merged images suggest that Mob1B and NDR1 (Fig. 3*D*) or NDR2 (Fig. 3*G*) may have partially colocalized, interpretation of these results is difficult given the pan-cellular distribution of Mob1B.

We next performed a similar localization analysis with Mob2, the ~30-kDa protein that coimmunoprecipitated with both NDR1 and NDR2 (Fig. 2*A*). When expressed alone, Mob2 accumulated within the nucleus but was also observed within the cytoplasm (Fig. 3*H*). Coexpression of Mob2 and NDR1 (Fig. 3, *I–K*) or NDR2 (Fig. 3, *L–N*) dramatically altered Mob2 distribution. Under these conditions, Mob2 was mostly cytoplasmic with strong perinuclear staining (Fig. 3, *I* and *L*). Likewise, NDR1 exhibited reduced nuclear accumulation and more prominent cytoplasmic speckles (Fig. 3*J*), whereas NDR2 remained mostly cytoplasmic (Fig. 3*M*). The merged image demonstrates that NDR1 and Mob2 colocalized within the cytoplasm, particularly within perinuclear regions (Fig. 3*K*). Likewise, NDR2 and Mob2 colocalized predominantly in perinuclear regions but also throughout the cytoplasm (Fig. 3*N*). Thus, coexpression of NDR1 and Mob2 results in NDR1 redistribution from the nucleus (Figs. 1*C* and 3*C*) to the cytoplasm (Fig. 3*J*). Furthermore, NDR1 or NDR2 coexpression results in Mob2 relocalization to perinuclear regions (Fig. 3, compare *I* and *L* with *H*).

*Differential Binding of NDR Kinases to Mob1B and Mob2*—The above analysis demonstrates that NDR1 and NDR2 colocalize with Mob2 in human cell lines. To extend these findings, we purified FLAG-NDR1 or FLAG-NDR2 from 293T cells following cotransfection with plasmids encoding GFP, GFP-Mob1B, or GFP-Mob2. Whole cell extracts were analyzed by anti-FLAG (Fig. 4*A*) and anti-GFP (Fig. 4*B*) Western blot to ensure equivalent expression of the respective FLAG and GFP fusion proteins. Following anti-FLAG affinity purification, a significant amount of Mob2 was coeluted with NDR1 and NDR2 (Fig. 4*D*). Mob1B also was coeluted with NDR2 (Fig. 4*D*) and, to a lesser extent, with NDR1 (see longer exposure in Fig. 4*E*). These results confirm that NDR1 and NDR2 bind both Mob1B and Mob2. Interestingly, the kinases appear to bind Mob2 more tightly than Mob1B in cell extracts, a finding consistent with our microscopy studies (Fig. 3). We also observed that the Mob1B-NDR1 interaction is significantly weaker than the Mob1B-NDR2 interaction, a finding consistent with our initial immunoprecipitations (Fig. 2*A*).

Subsequently, we performed *in vitro* kinase reactions to examine the functional consequence of Mob1B and Mob2 association with NDR1 and NDR2. Mob2 dramatically stimulated autophosphorylation of NDR2 and, to an apparently lesser extent, NDR1 (Fig. 4*F*). The size of the lower band is consistent with GFP-Mob2

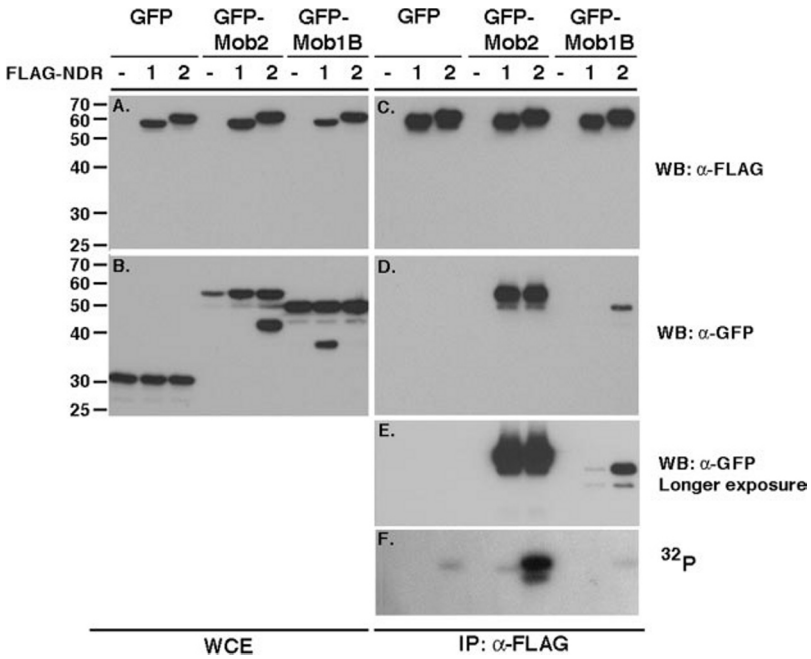


FIG. 4. **Directed coimmunoprecipitation confirms NDR1 and NDR2 interactions with Mob1B and Mob2.** 293T cells were transiently transfected with plasmids encoding GFP, GFP-Mob1B, or GFP-Mob2 plus or minus (−) plasmids encoding FLAG-NDR1 or FLAG-NDR2. Whole cell extracts (*WCE*) were analyzed by Western blotting using anti-FLAG M2 (*A*) or anti-GFP antibodies (*B*). GFP migrated at ~30 kDa, whereas full-length GFP-Mob2 and GFP-Mob1B migrated at ~55 and ~50 kDa, respectively. The smaller GFP-reactive bands represent C-terminal truncations. WCE were subsequently immunoprecipitated with the anti-FLAG affinity matrix. Immunoprecipitated proteins were eluted with the FLAG peptide and analyzed by anti-FLAG (*C*) and anti-GFP (*D* and *E*) Western blotting. GFP-Mob2 was specifically coimmunoprecipitated with FLAG-NDR1 and FLAG-NDR2. GFP-Mob1B was specifically coimmunoprecipitated with FLAG-NDR2 (*D*) and, to a lesser extent, with FLAG-NDR1 (*E*). *F*, the functional significance of the NDR-Mob interactions was analyzed by an *in vitro* kinase reaction. Autophosphorylation of NDR2 was weakly observed when NDR2 was purified alone or in the presence of GFP-Mob1B, yet was dramatically stimulated in the presence of GFP-Mob2. NDR1 autophosphorylation was only observed in the presence of GFP-Mob2.

(Fig. 4*F*; see also Fig. 5*B*), suggesting that Mob2 itself may be a substrate of NDR2. Mob1B did not stimulate NDR1 or NDR2 autophosphorylation in our assay, although given that it was significantly less abundant than Mob2 in our enzyme preparations, we cannot conclude that Mob1B does not stimulate NDR1 or NDR2 kinase activity. Indeed, the stringent purification conditions (500 mM NaCl, 1% Triton X-100) may have promoted disassociation of an otherwise stable and functionally significant NDR1- or NDR2-Mob1B interaction.

*Transphosphorylation by NDR1- and NDR2-Mob2 Complexes*—Previous studies have noted that GST-NDR1 or hemagglutinin-NDR1 fail to transphosphorylate generic kinase substrates (1). Because Mob2 association stimulates NDR1 and NDR2 autophosphorylation, we next tested these preparations for transphosphorylation activity. To determine whether NDR1- or NDR2-Mob2 complexes could catalyze transphosphorylation of heterologous substrates, we transiently expressed wild-type (WT) or catalytically inactive (KD) FLAG-NDR1 and FLAG-NDR2 along with GFP-Mob2. For these experiments, we treated cells with 1 μM okadaic acid prior to affinity purification, which has been shown to dramatically stimulate hemagglutinin-NDR1 activity (2, 4). This treatment also stimulates the activity of FLAG-NDR2 (data not shown). We first examined the purity of our enzyme preparations by SDS-PAGE and Simply Blue staining. This analysis demonstrated that NDR1 and NDR2 bound Mob2 in a 1:1 ratio (Fig. 5*A*). Furthermore, the catalytic activity of NDR1 and NDR2 was not required for Mob2 association (Fig. 5*A*).

*In vitro* kinase reactions were performed next using the above enzyme preparations and dephosphorylated MBP as substrate. NDR2 readily phosphorylated the ~18-kDa MBP as well as the ~24-kDa inactivated λ-phosphatase present within the MBP preparation (Fig. 5*B*). Two additional low abundance contaminants were phosphorylated by NDR2. These contaminants originated from the MBP preparation, because they were not observed in reactions in which MBP was omitted (data not shown). NDR2 autophosphorylation and Mob2 transphosphorylation were also observed (Fig. 5*B*), consistent with our previous findings (Fig. 4*F*). Reactions containing KD NDR2 exhibited negligible kinase activity, demonstrating that the NDR2 preparations were relatively pure.

NDR1 also phosphorylated MBP, albeit to a lesser extent than NDR2 (Fig. 5*B*). Interestingly, reactions containing KD NDR1 exhibited significantly more kinase activity than those containing KD NDR2. Given that significantly more Hsp90 copurified with KD NDR1 (Fig. 5*B*), the background enzymatic activity was probably the result of unknown kinase(s) associated with a subpopulation of Hsp90. Importantly, MBP transphosphorylation was invariably higher following incubation with WT NDR1 than with KD NDR1 (data not shown).

## DISCUSSION

Here, we present molecular characterization of the human NDR2 serine-threonine kinase. Furthermore, we identified a new family of human kinase regulators via their interactions with the NDR1 and NDR2 serine-threonine kinases. Mob2 colocalizes with NDR1 and NDR2 in human cell lines and binds NDR1 and NDR2 *in vitro*. Importantly, the Mob2 interaction dramatically stimulates NDR1 and NDR2 kinase activity.

In contrast to NDR1, which is predominantly nuclear, NDR2 is localized predominantly to the cytoplasm. This observation is intriguing given the extremely high degree of sequence identity between the two enzymes. The punctate cytoplasmic distribution of FLAG-NDR2 and GFP-NDR2 (and to a lesser extent FLAG- and GFP-NDR1) suggests that a population of NDR2 may be restricted to a specific subcellular compartment.

Mob1B and Mob2 were identified as NDR1 and NDR2 binding partners. Transient transfection studies demonstrated that

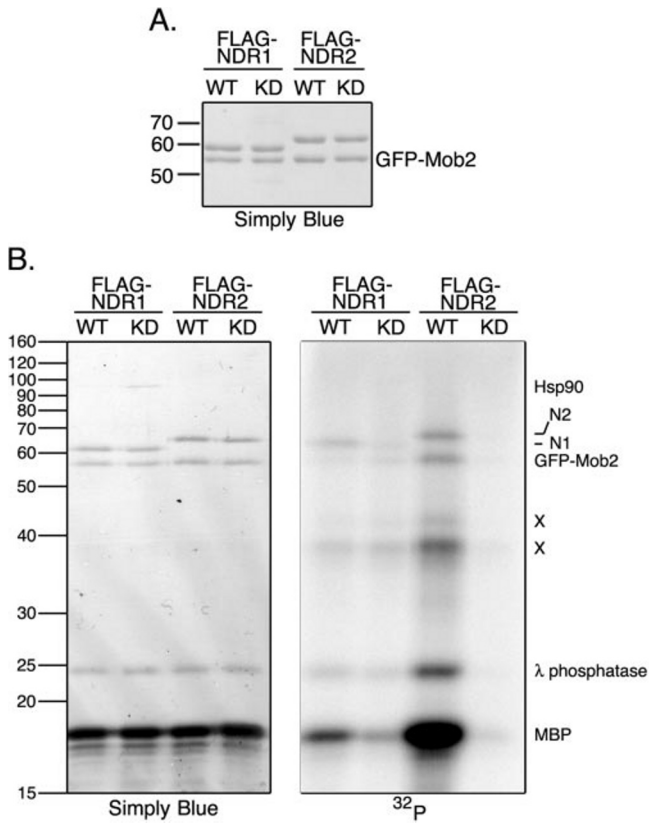


FIG. 5. **Transphosphorylation by NDR1- and NDR2-Mob2 complexes.** *A*, 293T cells were transiently transfected with WT or KD FLAG-NDR1 and FLAG-NDR2 expression vectors along with pGFP-Mob2. Transfected cells were pulsed with 1 $\mu$M okadaic acid prior to lysis and immunoprecipitation. SDS-PAGE and Simply Blue staining demonstrate that GFP-Mob2 was purified in a 1:1 ratio with FLAG-NDR1 and FLAG-NDR2. The catalytic activity of NDR1 and NDR2 is not required for this association, because GFP-Mob2 was also purified with KD enzymes. *B*, *in vitro* kinase reactions were performed using the enzyme preparations shown in *A* with dephosphorylated MBP as substrate. Reactions were resolved by SDS-PAGE, stained with Simply Blue, and analyzed by exposure to a PhosphorImager. Transphosphorylation of MBP is observed in reactions containing WT NDR2 (N2) and, to a lesser extent, NDR1 (N1). Transphosphorylation of GFP-Mob2 is also observed in reactions containing WT NDR2 as well as several low abundance proteins (*X*) and the ~24-kDa λ phosphatase. Interestingly, significantly more Hsp90 copurified with KD NDR1, which probably accounts for the increased background kinase activity associated with KD NDR1. MBP phosphorylation was invariably greater upon incubation with WT NDR1 than KD NDR1 (data not shown).

a fraction of Mob1B copurifies with NDR1 or NDR2 following immunoprecipitation under stringent conditions (500 mM NaCl, 1% Triton X-100). Mob2 tightly associates with NDR1 and NDR2 and is affinity-purified in a 1:1 stoichiometry with the kinases. At present, it is unclear whether the NDR kinases genuinely have a higher affinity for Mob2 than Mob1B. Indeed, it is possible that the interaction between NDR1 or NDR2 and Mob2 is salt- and/or detergent-sensitive or that the GFP moiety interferes with the interaction. We also demonstrated that NDR1 and NDR2 partially colocalize with Mob2 in human cell lines with the caveat that this analysis was performed with heterologously expressed proteins. Interestingly, the coexpression of Mob2 with NDR1 or NDR2 affects the subcellular localization of both proteins, and colocalization is mostly observed in regions surrounding the nucleus.

*In vitro* kinase reactions demonstrated that Mob2 dramatically stimulates the kinase activity of NDR1 and NDR2. We have shown that NDR1/2-Mob2 complexes are capable of both autophosphorylation and transphosphorylation of heterologous substrates. Interestingly, NDR2 is significantly more active than NDR1. At present, it is unclear whether NDR kinase activity is governed solely by primary sequence determinants or whether differential post-translational modifications account for increased NDR2 activity. In this respect, it is intriguing that NDR2 invariably migrates more slowly than NDR1 following SDS-PAGE despite the fact that the calculated molecular mass of NDR1 exceeds that of NDR2 by ~187 Da.

Recently, Wu and colleagues (17) performed differential display PCR to identify genes preferentially expressed in human hepatocellular carcinomas (17). The authors cloned a 2520-bp mRNA that they named *HCCA2* (hepatocellular carcinoma-associated gene 2) (GenBank™ accession number AF206328) and determined that *HCCA2* mRNA was widely expressed in adult human tissues. Importantly, *HCCA2* mRNA was detected in 79% (34/43) of primary hepatocellular carcinoma tissue samples but not in normal surrounding tissues. Furthermore, the expression of *HCCA2* mRNA was correlated with Ki-67 protein expression and with tumor capsule invasion. The authors identified an ORF encoding a protein of ~50 kDa within the HCCA2 mRNA (HCCA2 protein, GenBank™ accession number AAL74055) and developed rabbit polyclonal antiserum against the C-terminal 160 amino acids of HCCA2 fused to GST. This antiserum detected a ~50-kDa protein in 293 extracts transiently transfected with a pcDNA.3 vector containing the full-length HCCA2 cDNA but not in untransfected cell lysates. Western blot analysis of other samples either was not performed or was not reported. Interestingly, the *HCCA2* mRNA also encodes an overlapping (but entirely distinct) ORF that was not described by Wu and colleagues (17). This alternate ORF encodes the Mob2 protein described here (GenBank™ accession number NP_443741). In our opinion, it is currently unclear whether the *HCCA2* mRNA encodes one (Mob2) or both (Mob2 and HCCA2) proteins. In light of our analysis, it is tempting to reinterpret this report as evidence that Mob2 expression and thus NDR activation are associated with hepatocellular carcinoma development or progression.

The work presented here provides the first documentation of a serine-threonine kinase stimulated by a human Mob homologue. The proteins identified here are homologous to the *S. cerevisiae* Mob1 and Mob2 proteins (scMob1, scMob2). scMob1 and scMob2 were initially identified via a yeast two-hybrid interaction with the Mps1 serine-threonine kinase (hence, the name Mob, Mps One Binder) (18). *MOB1* is an essential budding yeast gene required for cytokinesis and mitotic exit (18, 19). Aside from Mps1, scMob1 also binds the Dbf2 serine-threonine kinase (20) and regulates Dbf2 catalytic activity (3). scMob2 also forms a complex with the NDR family member Cbk1 and is important for maintaining polarized growth and regulation of the daughter cell-specific transcription factor, AceII (21). Interestingly, *Schizosaccharomyces pombe* Mob1 and Mob2 have been shown to interact with the fission yeast NDR kinase family members Sid2 and Orb6, respectively (22, 23). Taken together, our results show that Mob regulation of NDR activity has been conserved from yeast to humans.

It was previously hypothesized that scMob1 may activate Dbf2 by inducing a conformational switch analagous to cyclin-mediated activation of Cdks (3). Recently, the crystal structure of human Mob1A (BAB14525) was solved (Protein Data Base accession number 1PI1) (14). Of note, Mob1A is ~95% identical to Mob1B described here. The Mob1A structure revealed a negatively charged flat surface that is conserved among all of the Mob proteins that probably mediates electrostatic interactions with kinase binding partners (14). Although the structure of Mob1A does not resemble that of cyclins, cocrystal studies of Mob-NDR complexes might lend support to the cyclin-Cdk analogy. Regardless of the biophysical mechanism of activa-

tion, Mob proteins are conserved kinase-activating subunits. A sequence analysis demonstrated that the human genome contains seven *Mob* genes (data not shown). It will be interesting to determine whether other Mob proteins also regulate human NDR1, NDR2, or other members of the NDR kinase family. Given that NDR1, NDR2, and Mob2 have been implicated in melanomas, aggressive ductal carcinomas *in situ*, B-cell lymphomas, and hepatocellular carcinomas, molecular insight into the functions of the NDR kinases may lead to new therapeutic opportunities for the treatment of human cancers.

*Acknowledgment*—We thank Lynne Lacomis for help with mass spectrometry.

REFERENCES

1. Millward, T., Cron, P., and Hemmings, B. A. (1995) *Proc. Natl. Acad. Sci. U. S. A.* **92,** 5022–5026
2. Millward, T. A., Hess, D., and Hemmings, B. A. (1999) *J. Biol. Chem.* **274,** 33847–33850
3. Mah, A. S., Jang, J., and Deshaies, R. J. (2001) *Proc. Natl. Acad. Sci. U. S. A.* **98,** 7325–7330
4. Tamaskovic, R., Bichsel, S. J., Rogniaux, H., Stegert, M. R., and Hemmings, B. A. (2003) *J. Biol. Chem.* **278,** 6710–6718
5. Millward, T. A., Heizmann, C. W., Schafer, B. W., and Hemmings, B. A. (1998) *EMBO J.* **17,** 5913–5922
6. Hauschild, A., Engel, G., Brenner, W., Glaser, R., Monig, H., Henze, E., and Christophers, E. (1999) *Oncology* **56,** 338–344
7. Adeyinka, A., Emberley, E., Niu, Y., Snell, L., Murphy, L. C., Sowter, H., Wykoff, C. C., Harris, A. L., and Watson, P. H. (2002) *Clin. Cancer Res.* **8,** 3788–3795
8. Tamaskovic, R., Bichsel, S. J., and Hemmings, B. A. (2003) *FEBS Lett.* **546,** 73–80
9. Suzuki, T., Shen, H., Akagi, K., Morse, H. C., Malley, J. D., Naiman, D. Q., Jenkins, N. A., and Copeland, N. G. (2002) *Nat. Genet.* **32,** 166–174
10. Limon, A., Devroe, E., Lu, R., Ghory, H. Z., Silver, P. A., and Engelman, A. (2002) *J. Virol.* **76,** 10598–10607
11. Devroe, E., Engelman, A., and Silver, P. A. (2003) *J. Cell Sci.* **116,** 4401–4408
12. Erdjument-Bromage, H., Lui, M., Lacomis, L., Grewal, A., Annan, R. S., McNulty, D. E., Carr, S. A., and Tempst, P. (1998) *J. Chromatogr. A.* **826,** 167–181
13. Winkler, G. S., Lacomis, L., Philip, J., Erdjument-Bromage, H., Svejstrup, J. Q., and Tempst, P. (2002) *Methods* **26,** 260–269
14. Stavridi, E. S., Harris, K. G., Huyen, Y., Bothos, J., Verwoerd, P. M., Stayrook, S. E., Pavletich, N. P., Jeffrey, P. D., and Luca, F. C. (2003) *Structure* **11,** 1163–1170
15. Thompson, J. D., Higgins, D. G., and Gibson, T. J. (1994) *Nucleic Acids Res.* **22,** 4673–4680
16. Gouet, P., Courcelle, E., Stuart, D. I., and Metoz, F. (1999) *Bioinformatics* **15,** 305–308
17. Wang, Z. X., Wang, H. Y., and Wu, M. C. (2001) *Br. J. Cancer* **85,** 1162–1167
18. Luca, F. C., and Winey, M. (1998) *Mol. Biol. Cell* **9,** 29–46
19. Luca, F. C., Mody, M., Kurischko, C., Roof, D. M., Giddings, T. H., and Winey, M. (2001) *Mol. Cell Biol.* **21,** 6972–6983
20. Komarnitsky, S. I., Chiang, Y. C., Luca, F. C., Chen, J., Toyn, J. H., Winey, M., Johnston, L. H., and Denis, C. L. (1998) *Mol. Cell Biol.* **18,** 2100–2107
21. Weiss, E. L., Kurischko, C., Zhang, C., Shokat, K., Drubin, D. G., and Luca, F. C. (2002) *J. Cell Biol.* **158,** 885–900
22. Hou, M. C., Wiley, D. J., Verde, F., and McCollum, D. (2003) *J. Cell Sci.* **116,** 125–135
23. Hou, M. C., Salek, J., and McCollum, D. (2000) *Curr. Biol.* **10,** 619–622